ISSN 0036-0295, Russian Metallurgy (Metally), Vol. 2017, No. 10, pp. 842–850. © Pleiades Publishing, Ltd., 2017.
Original Russian Text © V.N. Serebryany, M.A. Khar'kova, G.S. D'yakonov, V.I. Kopylov, S.V. Dobatkin, 2017, published in Deformatsiya i Razrushenie Materialov, 2017, No. 2, pp. 25–33.

STRUCTURE AND PROPERTIES OF THE DEFORMED STATE

Shear Bands and Anisotropy of the Mechanical Properties of an MA2-1pch Magnesium Alloy after Equal-Channel Angular Pressing

V. N. Serebryany[a, *], M. A. Khar'kova[a], G. S. D'yakonov[b], V. I. Kopylov[c], and S. V. Dobatkin[a, d]

[a] *Baikov Institute of Metallurgy and Materials Science, Russian Academy of Sciences, Leninskii pr. 49, Moscow, 119334 Russia*

[b] *Ufa State Aviation Technical University, ul. K. Marksa 12, Ufa, 450000 Russia*

[c] *Physicotechnical Institute, Belarussian Academy of Sciences, ul. Kuprevicha 10, Minsk, 220141 Belarus*

[d] *National University of Science and Technology MISiS, Leninskii pr. 4, Moscow, 119049 Russia*

**e-mail: vns@imet.ac.ru*

Received May 25, 2016; in final form, October 12, 2016

Abstract—Effect of structure and texture on the anisotropy of the mechanical properties of the MA2-1pch magnesium alloy subjected to equal-channel angular pressing and subsequent annealing has been studied in two mutually perpendicular planes *Y* and *X* (along and across the pressing direction). The anisotropy of the mechanical properties is shown to be due to various orientations of shear bands and various types of texture inside the bands and outside them in planes *X* and *Y*.

Keywords: texture, shear bands, anisotropy of mechanical properties, equal-channel angular pressing, MA2-1pch magnesium alloy

DOI: 10.1134/S0036029517100214

1. INTRODUCTION

Equal-channel angular pressing (ECAP) is an efficient method of severe plastic deformation, which makes it possible to substantially enhance the mechanical properties of metals and alloys as a result of refinement of a grain structure and a change in crystallographic texture [1, 2]. A specific feature of this method is the development of severe plastic deformation via simple shear in a sample when the joint of two mutually intersecting channels is passed with subsequent deformation localization in the planes inclined by 45°–60° to the initial sample pressing direction.

The ECAP process is frequently accompanied by a nonuniform intensity of shear strains along the cross section of a sample. Under given conditions of the contact friction between the channel walls and the sample surface, this nonuniformity is determined by temperature, the strain magnitude and rate, and by the competition between the ability to strain hardening and the effect of adiabatic heating in the severe deformation zone [3–5]. The peculiarities of the strain flow during ECAP can substantially influence the properties of magnesium alloys, which are characterized by wesk deformability. In [5, 6], the anisotropy of the mechanical properties of magnesium alloys after ECAP was not related to the orientation of shear bands. However, their appearance can lead to a change in the anisotropy of the properties in various planes of pressed samples [7] with subsequent microcrack formation along band boundaries and the fracture of a material during ECAP, as it was shown for the AZ31 magnesium alloy in [8].

The necessity of providing an increased level of the properties of semifinished products of magnesium alloys needs the study of the peculiarities of the structure and texture formation during ECAP. The aim of this work is to investigate the influence of the texture and the microstructure of the MA2-1pch alloy subjected to ECAP and subsequent annealing on the anisotropy of its mechanical properties.

2. EXPERIMENTAL

20 × 20 × 120-mm bars cut from hot-pressed rods of the MA2-1pch alloy (4.4% Al, 0.9% Zn, 0.4% Mn, 0.01% Cu) were subjected to ECAP deformation. ECAP was carried out at 245°C by route B_C at four passes in a die with an intersection angle of 90° and rotation of a sample by 90° by the axis after each pass (Fig. 1). Subsequent recrystallization annealing was carried out at 375°C for 1 h upon cooling in air.

After ECAP and annealing, longitudinal and transverse samples were cut out of two planes of the bars, namely, the end perpendicular to the pressing direc-

tion and the frontal plane oriented along the pressing direction (*X* and *Y*, respectively; Fig. 1). A microstructure was studied using conventional and polarized light and a Neophot-2 microscope with data processing by the Image Expert 3.3 program. A texture was studied with a DRON-7 X-ray texture diffractometer using Co$K\alpha$ radiation in reflection geometry and six incomplete pole figures {0004}, $\{10\bar{1}0\}$, $\{10\bar{1}1\}$, $\{10\bar{1}2\}$, $\{10\bar{1}3\}$, and $\{11\bar{2}0\}$ at the maximum slope $\rho_{max} = 70°$ and a step of 5° in angles ρ and β (ρ and β are the radial and azimuth angles in a pole figure, respectively).

An orientation distribution function (ODF), the ODF coefficients of expansion into a series of spherical functions, and the volume fractions of the main orientations were calculated by the statistical ridge estimate method [9] and approximation by a large number of Gaussian normal distributions [10]. (The quantitative texture analysis by approximation with a large number of Gaussian normal distributions enables an estimation of the generalized Schmid factors for active deformation system in a material.) The orientation factors were estimated using the relation [11]

$$M_i = \frac{1}{m_i}. \quad (1)$$

Here, m_i are the generalized Schmid factors of the basal, prismatic, and pyramidal slip and twinning determined by the expression

$$m_i = \sum_{j=1}^{p} m_{ij} W_j, \quad (2)$$

where m_{ij} is the orientation Schmid factor calculated for the *i*th slip system and the *j*th texture component, W_j is the volume fraction of the *j*th texture component, and *p* is the number of texture components.

The texture and the microstructure of the alloy also were studied by electron backscatter diffraction (EBSD) using a Quanta 600 FEG field-emission scanning electron microscope [12]. The scanning plane in a sample was perpendicular to the pressing direction. The Schmid factor distribution over grains for the main deformation systems of the alloy was calculated using orientation maps of the microstructure and the TSL OIM Analysis 5 software package.

Uniaxial tensile tests were carried out at on Instron-1165 testing machine at room temperature and a strain rate of 6×10^{-3} s^{-1} using plane dumbbell specimens with a gage size of 1 × 6 × 14 mm. The error of determining the mechanical properties was 10%.

The anisotropy of the strength properties was estimated according to the Taylor–Bishop–Hill model for the case of the monoclinic symmetry of a specimen [13–15] revealed after ECAP in plane *X* perpendicular to the pressing direction. This method was based on calculating the external deformation energy and the related Taylor factor $M(q, g)$ for each grain, where *q* is the parameter determining the deformation tensor and *g* is the grain orientation. Then, the Taylor factor was averaged over all orientations using ODF $f(g)$,

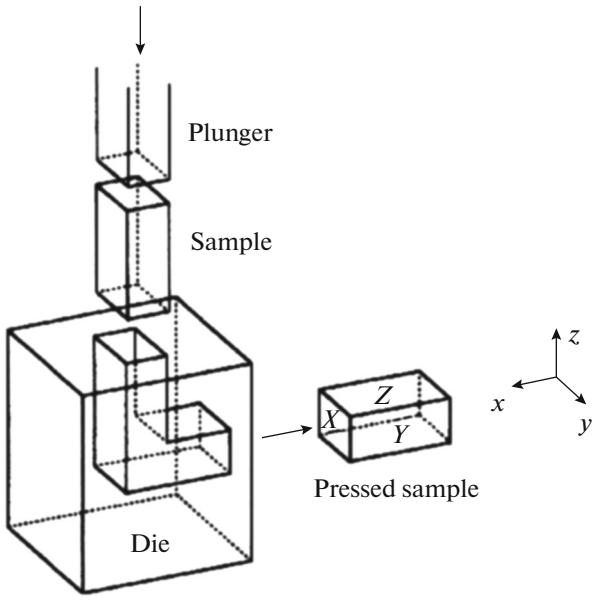

Fig. 1. Scheme of ECAP.

$$\bar{M}(q) = \int M(q,g) f(g). \quad (3)$$

We expand $f(g)$ and $M(q, g)$ into a series in spherical harmonics $T_l^{\mu\nu}(g)$ of monoclinic symmetry [14, 15] and the latter function into a power series in *q* and rewrite integral (3) in the form

$$\bar{M}(q,\alpha) = \sum_{l}\sum_{\mu}\sum_{\nu} \frac{m_l^{\mu\nu}(q) C_l^{\mu\nu}}{2l+1} \cos\nu\alpha. \quad (4)$$

Here, α is the angle between the tensile direction and the axis of the coordinate system lying in the specimen plane, $C_l^{\mu\nu}$ are the ODF coefficients of expansion into a series in spherical harmonics determined from an analysis of the experimental pole figures by the statistical ridge estimate method [9], and $m_l^{\mu\nu}$ are the coefficients of expansion of the Taylor factor into a series in spherical harmonics $T_l^{\mu\nu*}$ of the monoclinic symmetry calculated by formula [15]

$$m_l^{\mu\nu}(q) = (2l+1)\int M(q,g) T_l^{\mu\nu*}(g) dg. \quad (5)$$

For the calculation, the input parameters were the critical resolved shear stresses on possible acting slip and twinning systems providing material forming during tensile deformation.

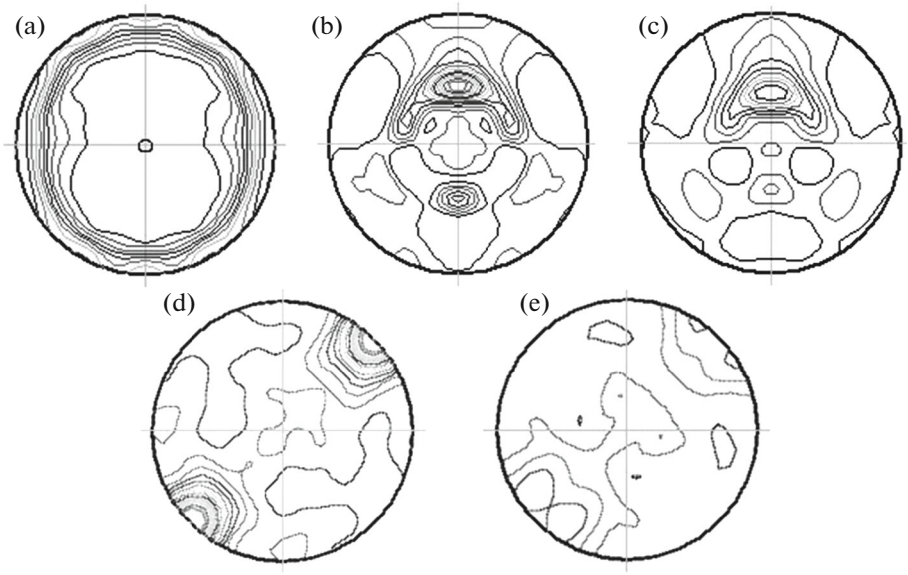

Fig. 2. (0004) pole figures in planes (a–c) *X* and (d, e) *Y* of the MA2-1pch alloy: (a) initial hot-pressed state, (b, d) after ECAP, and (c, e) after ECAP and annealing at 375°C, 1 h.

Experimental parameter q takes value $q_{\min}$ and minimizes the average Taylor factor. Then, in a particular case, we can determine anisotropy coefficients K_a of the properties of the alloy in two mutually orthogonal directions for planes *X* and *Y* by formula (0, 90 are arbitrary denotations of the orthogonal directions in the plane)

$$K_a = \frac{M(q_{\min,}0)}{M(q_{\min,}90)}. \quad (6)$$

We assumed that the plastic deformation of the magnesium alloy during uniaxial tension at room temperature was provided by the action of basal {0001}, prismatic $\{10\bar{1}0\}$, and pyramidal $\{10\bar{1}1\}$ dislocation slips along direction $\langle 11\bar{2}0\rangle$ and by pyramidal sliding $\{11\bar{2}2\}\langle 11\bar{2}\bar{3}\rangle$ and twinning $\{10\bar{1}2\}\langle\bar{1}011\rangle$ [15–17]. The critical resolved shear stresses in these deformation systems were estimated using the techniques described in [15, 18] by analyzing stress–strain curves and the evolution of a microstructure and texture during tension.

3. RESULTS AND DISCUSSION

3.1. Texture of the Alloy

The primary texture of the alloy contains a set of main orientations, which are characteristic of hot-pressed rods with predominant preferred directions $\langle 10\bar{1}0\rangle$ and $\langle 11\bar{2}0\rangle$ parallel to the pressing directions of the alloy (Fig. 2). The texture is fairly sharp and the volume fraction of the textureless component is 0.55 (Table 1).

The sharp prismatic texture of the primary state changes after ECAP at 245°C to a scattered texture inclined at an angle ≈45° to the pressing direction of the basal texture as a result of severe shear deformation in the planes disposed at an angle of ≈45° to the pressing direction (Fig. 2). The volume fraction of the textureless component increased to 0.76 (Table 1). Subsequent annealing at 375°C for 1 h did not change the type of scattered inclined basal texture formed after ECAP. However, the degree of texture scatter increased: the volume fraction of the textureless component was 0.85.

Prismatic slip is the most active deformation system of the alloy in the initial state, and its Schmid factor is maximal (Table 1). After ECAP, the most active deformation system is basal slip; its Schmid factor is higher than the initial one by a factor of more than two, and the activity of other deformation systems decreases as compared to the initial state. Subsequent annealing weakly changed the activity of the main deformation systems (Table 1).

3.2. Microstructure of the Alloy

The microstructure of the alloy in the initial state is homogeneous in the cross section of a sample; the grain size is 8–15 μm (average grain size is 12.4 μm). After ECAP, shear bands appear in the microstructure. In plane *X*, the bands are oriented along direction *y*; in plane *Y*, they are directed at an angle of 45°–55° to the pressing direction (Fig. 3). Similar shear bands were revealed in an AZ31B alloy after ECAP by an optical method [5].

Table 1. Main orientations in the terms of Eulerian angles, the volume fractions of orientations, the Schmid factors, and the orientation factors for the deformation systems of the MA2-1pch alloy in various structural states

State	Eulerian angles (after Bunge), deg			W_j	$m_{i,\text{ bas}}$ (0001)[11$\bar{2}$0]	$m_{i,\text{ prism}}$ (10$\bar{1}$0)[11$\bar{2}$0]	$m_{i,\text{ pyram}}$ (11$\bar{2}$2)[11$\bar{2}\bar{3}$]	$m_{i,\text{ tw}}$ (10$\bar{1}$2)[$\bar{1}$011]
	φ_1	Φ	φ_2					
Initial	20	90	20	0.050	0.000	0.328	0.223	0.246
	131	90	0	0.088	0.000	0.289	0.223	0.249
	85	90	0	0.096	0.000	0.289	0.223	0.249
	135	90	20	0.050	0.000	0.328	0.223	0.249
	Textureless component			0.545	0.200	0.159	0.150	0.125
	Generalized Schmid factor				0.113	0.227	0.183	0.181
	Orientation factor				8.845	4.407	5.464	5.514
ECAP	91	45	40	0.122	0.313	0.164	0.200	0.133
	71	49	15	0.063	0.319	0.190	0.183	0.106
	Textureless component			0.759	0.20	0.159	0.150	0.125
	Generalized Schmid factor				0.228	0.161	0.160	0.125
	Orientation factor				4.391	6.195	6.250	7.986
ECAP + 375°C, 1 h	98	35	0	0.017	0.313	0.095	0.246	0.253
	80	45	30	0.041	0.289	0.144	0.204	0.136
	Textureless component			0.852	0.200	0.159	0.150	0.125
	Generalized Schmid factor				0.215	0.154	0.160	0.134
	Orientation factor				4.644	6.490	6.246	7.450

Abbreviations bas, prism, and pyram stand for basal, prismatic, and pyramidal slip systems, respectively; tw, for twinning.

According to orientation maps, prismatic components dominate in the initial state in the alloy microstructure (Fig. 4a). After ECAP, grain orientations corresponding to inclined basal poles appear (Fig. 4b). They are predominantly located in the shear bands arranged in plane X perpendicular to the pressing direction and oriented along direction y. After annealing, bands almost disappear and most grains have the orientation of the inclined basal poles (Fig. 4c).

3.3. Schmid Factor Distributions of the Main Deformation Systems

In the initial state of the alloy, the Schmid factors for the basal and the prismatic deformation systems and the grain sizes along directions z and y in plane X change weakly. This state is characterized by an increased activity of prismatic slip (Schmid factor is close to 0.5); in this case, the grain size is ≈15 μm (Fig. 5a).

After ECAP, the Schmid factors of both deformation systems along direction z change nonmonotonically; in this case, the Schmid factors of prismatic slip outside shear bands is almost twice that of basal slip (Fig. 5b). It should be noted that the shear band width in plane X is 50–60 μm and that of the off-band space is approximately 20 μm. The average grain size along direction z changes weakly and is ≈2.3 μm (Fig. 5b). In direction y, the Schmid factors of basal and prismatic slip change slightly and their values for these deformation systems are approximately the same. This effect is mainly due to a change in the type and sharpness of texture in shear bands.

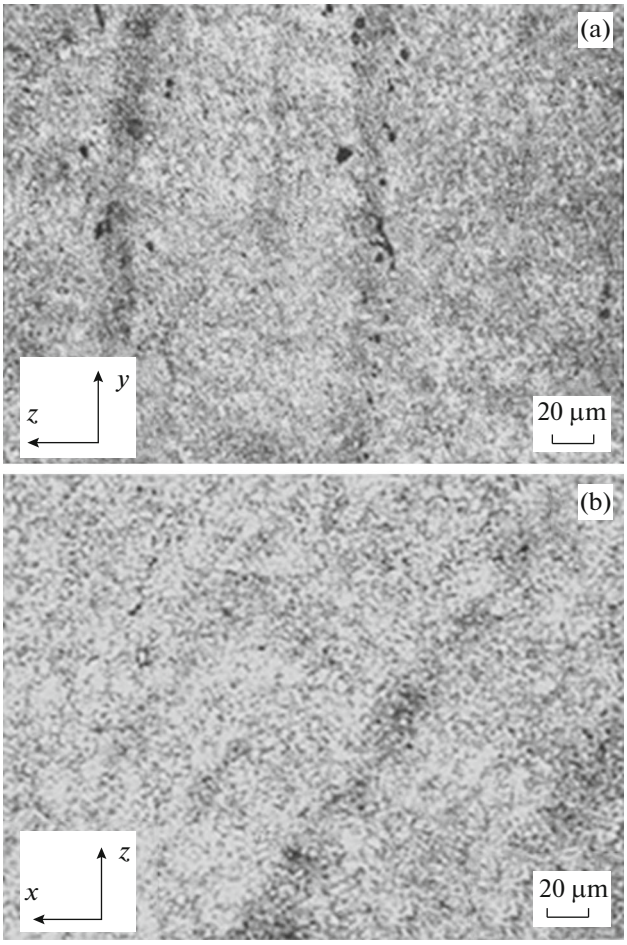

Fig. 3. Shear bands in planes (a) *X* and (b) *Y* of an MA2-1pch alloy bar after ECAP.

As a result of subsequent annealing, the distribution of the Schmid factors along direction *z* becomes more uniform, as in the initial state and after ECAP in direction *y*. The grain size changes weakly along the chosen directions; in this case, the grain size is larger (≈10.3 μm) than that after ECAP (Fig. 5c). These results along with the orientation maps of the microstructure show that shear bands almost disappear after annealing.

3.4. Anisotropy of the Mechanical Properties of the Alloy

In the initial state, the alloy has a weak anisotropy of the mechanical properties in plane *X*: the yield strength in two mutually orthogonal directions is 111 and 109 MPa; the ultimate strength is 255 and 264 MPa; and the relative elongation is 28.3 and 30.5%, respectively (Fig. 6). The anisotropy is significant in plane *Y*, in particular, for the yield strength: its value in the direction perpendicular to the pressing direction is twice as high as that along this direction.

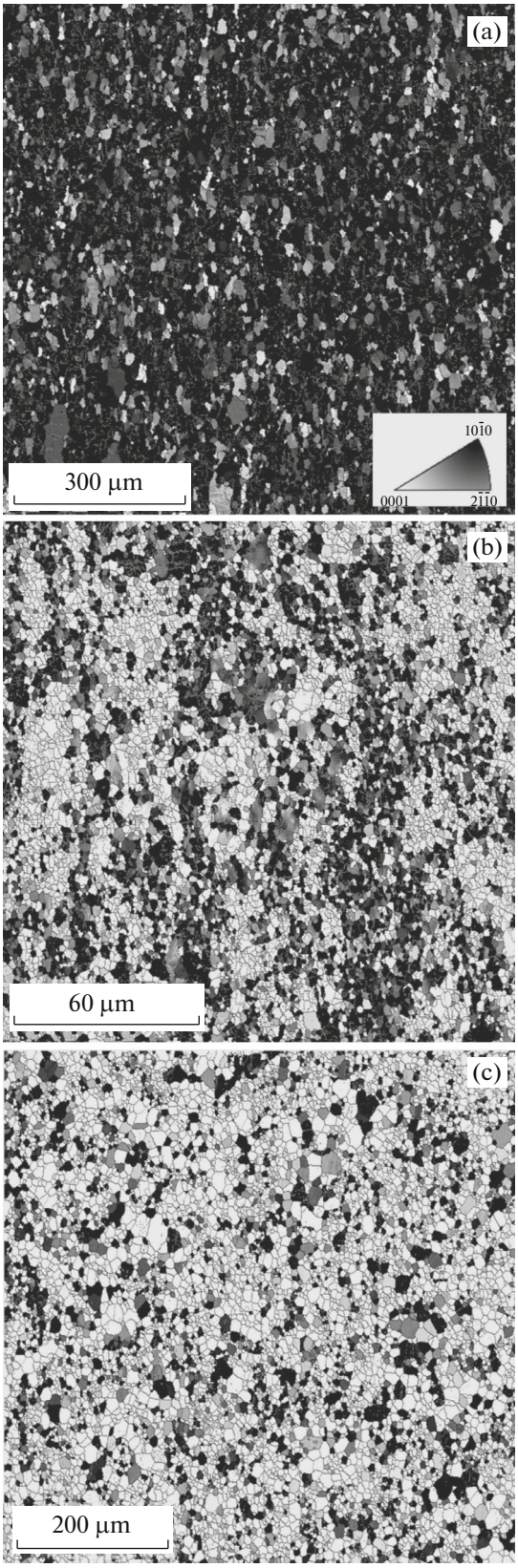

Fig. 4. Orientation maps of the MA2-1pch alloy microstructure in plane *X*: (a) initial hot-pressed state, (b) after ECAP, (c) after ECAP and annealing at 375°C, 1 h.

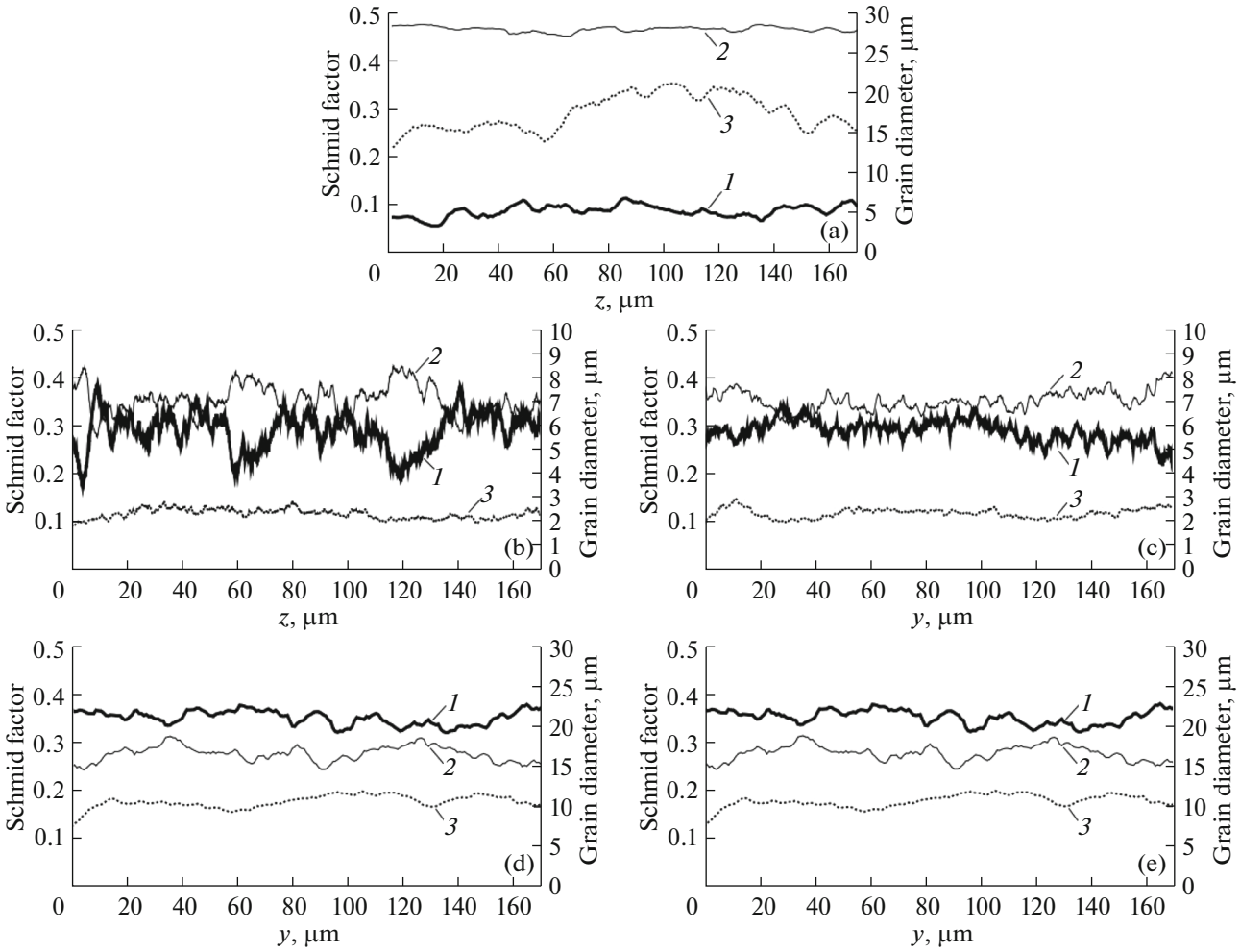

Fig. 5. Schmid factor distributions for (*1*) basal and (*2*) prismatic slip and (*3*) grain size distribution along directions *z* and *y* in plane *X*: (a) initial hot-pressed state, (b, c) after ECAP, and (d, e) after ECAP and annealing at 375°C, 1 h.

After ECAP, the anisotropy of the strength properties was observed in plane *X* (the yield strength is 110 and 214 MPa, the ultimate strength is 206 and 291 MPa, and the relative elongation is 16.3 and 25%, respectively); the anisotropy markedly decreased as a result of subsequent annealing. This anisotropy is almost absent after ECAP and annealing. After annealing, the anisotropy of the relative elongation is significantly smaller and the relative elongation increases noticeably.

3.5. Effect of the Texture Nonuniformity on the Anisotropy of the Mechanical Properties

The effect of the texture in shear bands and outside them (Fig. 7) in plane *X* on the anisotropy of the yield strength was calculated in terms of the Taylor model, assuming that basal, prismatic, and $\langle c + a \rangle$ pyramidal slip and twinning are operative during uniaxial tension [12–15].

The ratios of the critical resolved shear stresses of the acting deformation systems in shear bands and outside them in directions *x* and *y* were determined taking into account the changes in the Schmid factors due to a change of the texture and in the grain size for the twinning system (Fig. 6). Table 2 gives the calculated and experimental values of K_a and the critical resolved shear stresses for acting deformation systems. In accordance with the shear band sizes and the off-band space, we assumed that shear bands and the off-band space occupy 75 and 25% of the metal volume, respectively. The resulting calculated values of K_a were found by summing the values calculated for the alloy in shear bands and outside them with allowance for their volume fractions. It was found that the anisotropy of the yield strength in plane *X* of the alloy subjected to ECAP is determined to a significant degree

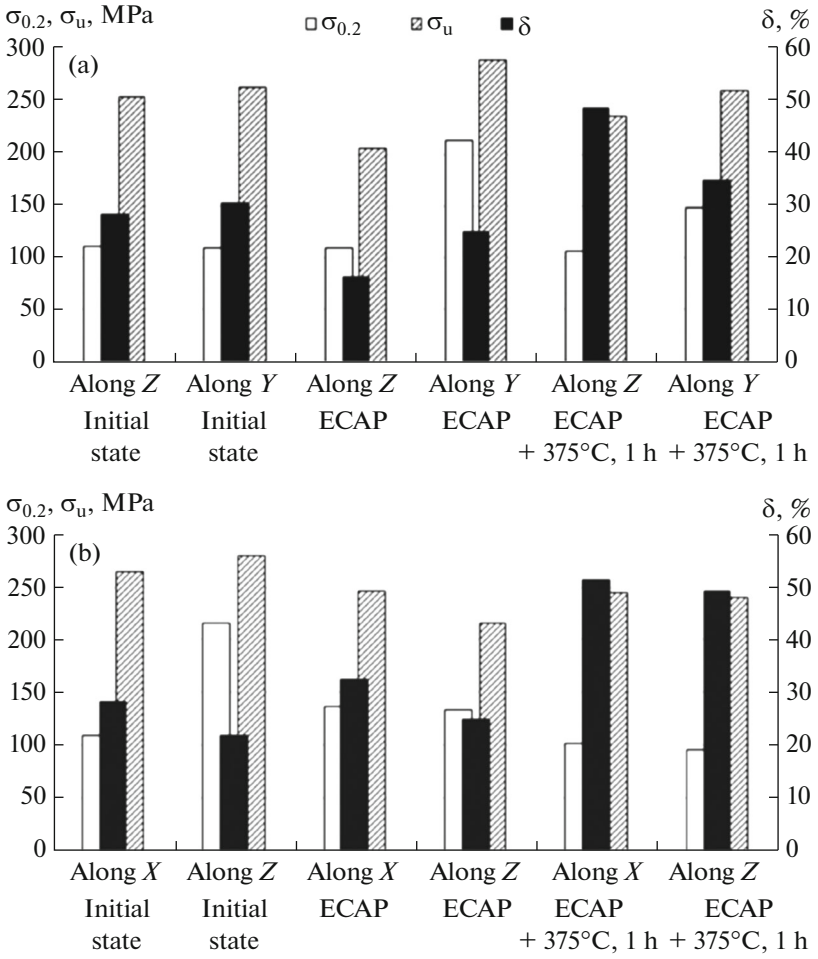

Fig. 6. Anisotropy of the mechanical properties of the MA2-1pch alloy in planes (a) *X* and (b) *Y* in the initial state and after ECAP and annealing at 375°C, 1 h.

by the orientation and the width of shear bands and by the type of anisotropy and its sharpness in shear bands and the off-band space. The coincidence of the calculated and the experimental values of K_a can be considered to be adequate. The complete coincidence of results is not attained supposedly because of that the

Table 2. Calculated ($K_{a,c}$) and experimental ($K_{a,ex}$) anisotropy coefficients and ratios of the critical resolved shear stresses of the MA2-1pch alloy in various structural states (plane *X*, Fig. 1)

State	Direction	$\sigma_{0.2}$, MPa	$\frac{\tau_{prism}}{\tau_{bas}}$	$\frac{\tau_{pyram}}{\tau_{bas}}$	$\frac{\tau_{tw}}{\tau_{bas}}$	$K_{a,c}$	$\Sigma K_{a,c}$	$K_{a,ex}$
Initial	Along *z*	111	0.25	1.25	0.75			
	Along *y*	110	0.25	1.25	0.75			
						1.00		1.01
ECAP	Along *z*	110/110	1.0/0.5	2.0/2.0	2.0/2.0			
	Along *y*	214/214	0.83/0.83	4.17/4.17	4.17/4.17			
						0.54/0.87	0.62	0.51
ECAP + annealing (375°C, 1 h)	Along *z*	107	1.11	2.78	1.67			
	Along *y*	148	1.67	5.56	3.33			
						0.79		0.72

Abbreviations bas, prism, pyram stand for basal, prismatic, and pyramidal slip systems, respectively; tw, for twinning; *x*, *y*, and *z* are the coordinate system axes normal to the corresponding planes in a bar (Fig. 1). Before and after slash, data for shear bands and outside them, respectively.

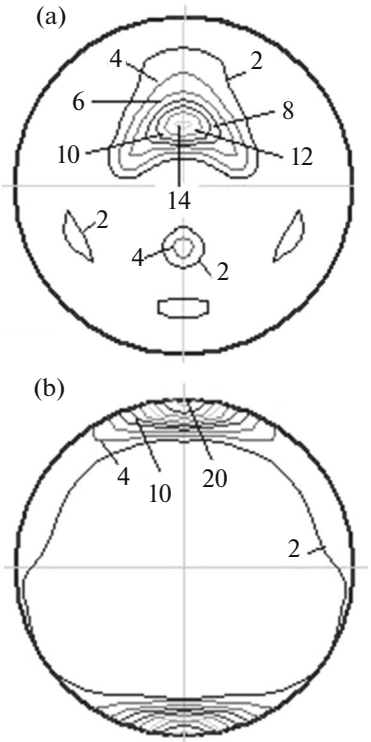

Fig. 7. (0004) pole figures of (a) shear bands and (b) regions outside them in the MA2-1pch alloy after ECAP.

anisotropy was calculated with allowance for only the texture factor. Similar analysis for planes *Y* is the subject of further investigations.

4. CONCLUSIONS

The anisotropy of the yield strength of the MA2-1pch alloy after ECAP is significantly due to the orientation of shear bands. The anisotropy is maximal at the end surfaces of a sample (in plane *X*), where shear bands are oriented along direction *y*. However, it is minimal in the pressing plane, since shear bands are inclined at the same angle to the pressing direction and to the perpendicular direction. The calculation of the plastic anisotropy in terms of the Taylor model using the textures in shear bands and outside them with allowance for the band widths and orientations confirm this assumption. After annealing, bands disappear and the anisotropy of the yield strength also significantly decreases. Thus, we were the first to explain the anisotropy of the yield strength in the face-end plane of the MA2-1pch magnesium alloy after ECAP by the orientation of shear bands and the texture formed in them.

ACKNOWLEDGMENTS

This work was supported by the Russian Foundation for Basic Research (project no. 15-03-02829_a) and the Ministry of Education and Science of the Russian Federation (state contract no. 14.A12.31.0001).

REFERENCES

1. V. M. Segal, V. I. Reznikov, V. I. Kopylov, D. A. Pavlik, and V. M. Malyshev, *Processes of Plastic Structure Formation of Metals* (Nauka i Tekhnika, Minsk, 1994).
2. R. Z. Valiev and I. V. Aleksandrov, *Nanostructured Materials Produced by Severe Plastic Deformation* (Logos, Moscow, 2000).
3. V. M. Segal, "Equal channel angular extrusion: from macromechanics to structure formation," Mater. Sci. Eng. A **271**, 322–333 (1999).
4. R. B. Figueiredo, M. T. R. Aguilar, and P. R. Cetlin, "Finite element modeling of plastic instability during ECAP processing of flow-softening materials," Mater. Sci. Eng. A **430**, 179–184 (2006).
5. D. C. Foley, M. Al-Maharbi, K. T. Hartwig, I. Karaman, L. J. Kecskes, and S. N. Mathaudhu, "Grain refinement vs. crystallographic texture: mechanical anisotropy in a magnesium alloy," Scripta Materialia **64**, 193–196 (2011).
6. M. Al-Maharbi, I. Karaman, I. J. Beyerlein, D. Foley, K. T. Hartwig, L. J. Kecskes, and S. N. Mathaudhu, "Microstructure, crystallographic texture, and plastic anisotropy evolution in an Mg alloy during equal channel angular extrusion processing," Mater. Sci. Eng. A **528**, 7616–7627 (2011).
7. V. N. Serebryany, G. S. D'yakonov, M. A. Khar'kova, V. I. Kopylov, and S. V. Dobatkin, "Study of the texture and the structure of the MA2-1pch magnesium alloy after ECAP and annealing by a quantitative X-ray diffraction texture analysis and backscattered electron diffraction," Zavod. Lab. **82** (3), 36–41 (2016).
8. F. Kang, J. T. Wang, and Y. Peng, "Deformation and fracture during equal channelangular pressing of AZ31 magnesium alloy," Mater. Sci. Eng. A **487**, 68–73 (2008).
9. V. N. Serebryany, S. F. Kurtasov, and M. A. Litvinovich, "Study of the ODF errors during reversal of pole figures using the statistical method of ridge estimations," Zavod. Lab. **73** (4), 29–35 (2007).
10. S. F. Kurtasov, "The technique of the quantitative analysis of the rolling textures of materials with the cubic symmetry of the crystal lattice," Zavod. Lab. **73** (7), 41–44 (2007).
11. V. N. Serebryany, S. V. Dobatkin, and V. I. Kopylov, "Effect of the texture and the microstructure of the MA2-1 alloy after equal channel angular pressing," Tekhn. Legkikh Splavov, No. 3, 28–35 (2009).
12. V. N. Serebryany, G. S. D'yakonov, V. I. Kopylov, G. A. Salishchev, and S. V. Dobatkin, "Texture and structure contribution to low-temperature plasticity enhancement of Mg–Al–Zn–Mn alloy MA2-1pch

after ECAP and annealing," Phys. Met. Metallogr. **114** (5), 448–456 (2013).

13. D. R. Thornburg and H. R. Piehler, "An analysis of constrained deformation by slip and twinning in hexagonal close packed metals and alloys," Metall. Trans. A **6**, 1511–1523 (1975).
14. H. J. Bunge, "Technological applications of texture analysis," Z. Metallkde **76**, 457–470 (1985).
15. V. N. Serebryany and N. N. Pozdnyakova, "Evaluation of the normal anisotropy coefficient in AZ31 alloy sheets," Russ. Metall. (Metally), No. 1, 58–64 (2009).
16. M. H. Yoo, "Slip, twinning, and fracture in hexagonal close-packed metals," Metall. Trans. A **12**, 409–418 (1981).
17. D. J. Bacon and V. Vitek, "Atomic-scale modeling of dislocations and related properties in the hexagonal close-packed metals," Metall. Mater. Trans. A **33**, 721–733 (2002).
18. V. N. Serebryany, T. M. Ivanova, V. I. Kopylov, S. V. Dobatkin, N. N. Pozdnyakova, V. A. Pimenov, and T. I. Savelova, "Effect of equal channel angular pressing and annealing conditions on the texture, microstructure and deformability of the MA2-1 alloy," Russ. Metall. (Metally), No. 4, 648–657 (2010).

Translated by Yu. Ryzhkov